• Basic Research •

Long non-coding RNA H19 knockout activates the SAHH/DNMT3b pathway and represses NLRP3 inflammasome expression in a diabetic rat model

Hui Chen, Yu-Hui Pang, Xiong-Ze Zhang, Nan-Ying Liao, Miao-Ling Li, Yu-Ying Ji, Lan Mi, Yu-Hong Gan, Yong-Yue Su, Feng Wen

State Key Laboratory of Ophthalmology, Zhongshan Ophthalmic Center, Sun Yat-sen University, Guangdong Provincial Key Laboratory of Ophthalmology and Visual Science, Guangdong Provincial Clinical Research Center for Ocular Diseases, Guangzhou 510060, Guangdong Province, China

Co-first Authors: Hui Chen and Yu-Hui Pang

Correspondence to: Feng Wen. State Key Laboratory of Ophthalmology, Zhongshan Ophthalmic Center, Sun Yat-sen University, 54 South Xianlie Road, Guangzhou 510060, Guangdong Province, China. wenfeng208@foxmail.com

Received: 2025-05-28 Accepted: 2026-08-06

Abstract

● **AIM:** To explore the regulatory effect of long non-coding RNA H19 on the Nod-like receptor protein 3 (NLRP3) inflammasome and its functional role in the progression of diabetic retinopathy (DR).

● **METHODS:** Wild-type and H19 knockout rats were subjected to a high-fat and high-sugar diet combined with streptozotocin injection to establish an *in vivo* diabetes mellitus (DM) model. *In vitro*, rat primary retinal microvascular endothelial (CP-R114) cells were cultured under high-glucose conditions to mimic the diabetic microenvironment. The MTS assay was performed to evaluate cell viability. Enzyme-linked immunosorbent assay (ELISA) was used to detect the levels of indicators related to glucose metabolism, lipid metabolism, oxidative stress, and inflammation in rat retinal tissues and CP-R114 cells. Hematoxylin and eosin (HE) staining was applied to observe the pathological morphological changes in retinal tissues. qRT-PCR was conducted to quantify the mRNA expression of H19, S-adenosylhomocysteine hydrolase (SAHH), and S-adenosylmethionine-dependent methyltransferase 3 beta (DNMT3b) in rat retinas. Western blotting and immunofluorescence staining were further utilized to detect the protein expression of SAHH, DNMT3b, NLRP3, Caspase-1, and interleukin (IL)-1β in retinal tissues.

● **RESULTS:** In DM model rats, H19 knockout significantly improved glucose and lipid metabolic disorders and alleviated oxidative stress. Notably, H19 deficiency effectively ameliorated retinal tissue injury. The expression levels of intercellular cell adhesion molecule-1 (ICAM-1), vascular endothelial growth factor (VEGF), and pro-inflammatory factors were markedly downregulated in H19-silenced DM rats. Mechanistically, H19 knockout upregulated the expression of SAHH and DNMT3b, while inhibiting the expression of NLRP3 inflammasome-associated proteins in DM rats. Consistent with the *in vivo* findings, H19 silencing suppressed NLRP3 inflammasome activation and elevated SAHH and DNMT3b expression in high-glucose-stimulated CP-R114 cells.

● **CONCLUSION:** This study demonstrates that H19 knockout alleviates DR progression in diabetic rats by activating the SAHH/DNMT3b signaling pathway and inhibiting NLRP3 inflammasome activation. Therefore, targeting H19 represents a promising novel therapeutic strategy for the clinical treatment of DR.

● **KEYWORDS:** SAHH/DNMT3b; NLRP3 inflammasome; long non-coding RNA H19; diabetic retinopathy; rat

DOI:10.18240/ijo.2026.11.04

Citation: Chen H, Pang YH, Zhang XZ, Liao NY, Li ML, Ji YY, Mi L, Gan YH, Su YY, Wen F. Long non-coding RNA H19 knockout activates the SAHH/DNMT3b pathway and represses NLRP3 inflammasome expression in a diabetic rat model. *Int J Ophthalmol* 2026;19(11):2122-2134

INTRODUCTION

Diabetes mellitus (DM) is a global health crisis, with the number of people affected by the disease expected to reach 380 million by 2050[1-2]. The glucose metabolism dysfunction in DM is believed to be the crucial pathological component that advances the complications that arise in the small blood vessels which can cause organ damage. These complications can lead to the onset of a plethora of

conditions including kidney disease, cardiovascular disease, and loss of vision[3-6]. When fluctuations in blood glucose levels excessively affect the micro-vessels in the eyes, they can lead to neuronal damage in the retina, a condition known as diabetic retinopathy (DR), which is a leading cause of blindness in adults[7-8]. The progression of DR is accompanied by pathological processes such as vascular leakage, macular edema, and neovascularization. Numerous theories have been proposed to explain the pathogenesis of DR, including polyol pathway activation, overproduction of advanced glycation end-products, oxidative stress, activation of protein kinase C, and inflammation[9].

The pathophysiology and progression of DR are considered to be modulated by the inflammatory response[10]. DR is marked by the infiltration of inflammatory cytokines in the retina's microenvironment; this action is correlated with the functional degeneration of the retina. It has been shown that inhibiting inflammatory infiltration can improve the outcome of this condition[11-12]. In the diabetic eye, NLR family pyrin domain containing 3 (NLRP3) inflammasome activation is promoted by factors such as the presence of reactive oxygen species (ROS) and cellular stress. This activation leads to the production and release of interleukin (IL)-1β and IL-18, which trigger pyroptosis of the retinal cells. The death and rupture of these cells cause further production of inflammatory cytokines, thereby accelerating the progression of DR[13]. An accumulation of research has validated the crucial function played by NLRP3 inflammasome in the pathological process of DR[14-15]. NLRP3 inflammasome inhibition hinders retinal microvascular dysfunction and alleviates DR progression[16].

Long non-coding RNAs (lncRNAs) majorly are significant factors in gene expression modulation and regulation of a variety of disease processes and physiological processes[17-18]. Numerous studies have investigated the functional role of lncRNA H19 in diseases[19], revealing its association with DR. For instance, H19 regulates inflammatory response in high-glucose-treated retinal endothelial cells[20-21]. Overexpression of H19 represses glucose-induced endothelial-mesenchymal transition and prevents DR disease advancement[22]. Moreover, the recent studies[23-27] revealed H19 participated in the modulation of the genome-wide DNA methylation of mice skeletal muscles, human cancer cells, and stem cells through interaction with S-adenosylhomocysteine hydrolase (SAHH). SAHH is a primary inhibitor of S-adenosylmethionine-dependent methyltransferases (DNMT), such as DNMT1, DNMT2, DNMT3a, and DNMT3b, it does so by binding to S-adenosine homocysteine (SAH)[28]. When H19 interacts with SAHH, it inactivates the enzyme, leading to SAH buildup. This sequence of events culminates in the inhibition of DNMT3b activity resulting in reduced DNA methylation levels[25-26]. Additionally, our preliminary experiments have found that DNMT3b silencing promotes expression levels of NLRP3 in retinal endothelial cells. Thus, we speculated that H19 may regulate NLRP3 inflammasome and SAHH/DNMT3b pathway to affect the progression of DR.

MATERIALS AND METHODS

Ethical Approval Protocols in this study were authorized by the Ethics and Committee Review Board of Sun Yat-sen University-Zhongshan Ophthalmic Center-Institutional (SYSU-ZOC IRB), ethics approval number O2022006.

Animals Sprague-Dawley (SD) male rats (150–180 g) from SPF Biotechnology Co., Ltd (Beijing, China) were used in this research. An H19 knockout (H19-KO) rat model with SD genetic background (weighting 150–180 g) was created by Cyagen Biosciences (Guangzhou, China) using CRISPR/Cas-mediated genome engineering. Rats were housed in specific pathogen free (SPF) housing, which had a 12h light/dark cycle.

Rat Model of Diabetes Mellitus To construct the rat DM model, the animals were fed a high-fat, high-sugar (HFHS) diet combined with streptozotocin (STZ). An HFHS diet was given to the rats for 8wk. Then the rats received an injection intraperitoneally of 30 mg/kg STZ on the 28th day of the challenge (Sigma-Aldrich, St. Louis, MO, USA) after a 20h fast. The rats (n=6) were randomly split into 4 groups: 1) wide type (WT): normal SD rats were fed a normal diet and a sodium citrate buffer (SSC) injection was administered; 2) H19-KO: H19-KO rats were fed a normal diet and an SSC injection was administered; 3) WT+STZ: SD rats were fed an HFHS diet and an STZ injection was administered; 4) H19-KO+STZ: H19-KO rats were fed an HFHS diet and an STZ injection was administered.

After modeling, the measurement of the mean fasting blood glucose levels was recorded with a Roche glucometer (Roche, Basel, Switzerland). Blood sugar levels greater than 7.8 mmol/L indicated successful modeling of the DM rats. The weight of the rats was measured. Anesthesia was induced in rats by intraperitoneal administration of 10% chloral hydrate (4 mL/kg). Blood samples were obtained using venipuncture from the retroorbital venous sinus. After centrifugation of the blood samples for 10min at 2500 rpm, the supernatants were obtained and stored at -70℃ for future usage. The right thigh hind limb muscles, liver, and retina tissues were excised from rats and kept at -70℃ for future usage.

Cell Culture Rat retinal microvascular endothelial cell line CP-R114 cells (Procell Life Science & Technology Wuhan, China) were cultured using endothelial cell medium (ECM; Sciencell, Carlsbad, CA, USA) with 10% fetal bovine serum (FBS; Gibco, Grand Island, NY, USA), 1% streptomycin/penicillin (Solarbio, Beijing, China), and incubated in an atmosphere of 5% CO_2 at 37℃. After being subjected to 12h

of starvation, the cells were cultured for 24h in a 30 mmol/L glucose solution to mimic high glucose conditions.

MTS Assay MTS assay was conducted to analyze cell survival using CellTiter 96® AQueous One Solution Cell Proliferation Assay (Promega, Madison, WI, USA). CP-R114 cells (1.0×10^5/mL) were plated and cultured in 6 well-plates until they reached 80% confluence. The cells were then incubated for an hour at 37°C with the MTS reagent. The absorbance value of each well was detected at 490 nm wavelength using a Multiskan Go microplate reader (Thermo Fisher Scientific, Waltham, MA, USA).

Cell Transfection To silence H19, small interference RNA (siRNA) targeting H19 (si-H19; 5'-GGCCTTCCTGAACACCTTA-3') and a scrambled siRNA control (si-NC; 5'-UUCUCCGAACGUGUCACGUTT-3') were bought from GeneChem (Shanghai, China). Following the transfection of CP-R114 cells with si-H19 or si-NC utilizing Lipofectamine™ RNAiMAX Transfection Reagent (Thermo Fisher Scientific), the cells were cultured for 48h before being collected for further use.

Enzyme-Linked Immunosorbent Assay Enzyme-linked immunosorbent assay (ELISA) kit was conducted for glucose metabolism, lipid metabolism, oxidative stress, and inflammation-related factor levels detection in rats or CP-R114 cells. Briefly, retinal tissue samples were collected, homogenized in an appropriate volume of precooled phosphate-buffered saline (PBS), and centrifuged to obtain the supernatants. The protein concentrations of the samples were determined, and the samples were appropriately diluted according to the manufacturer's instructions. Standards and prepared samples were added to the corresponding wells of ELISA plates and incubated according to the manufacturer's recommended conditions. After washing, the wells were sequentially incubated with the corresponding detection antibody and enzyme conjugate. Following repeated washing, the substrate solution was added and incubated in the dark until color development. The reaction was terminated by adding the stop solution, and the absorbance was measured at 450 nm using a microplate reader. The concentrations of the target factors were calculated based on the corresponding standard curves. In the present study, ELISA was used to quantify IL-1β, IL-6, tumor necrosis factor-α (TNF-α), intercellular adhesion molecule-1 (ICAM-1), and vascular endothelial growth factor (VEGF) in rat retinal tissues.

Products Used in Experiment Superoxide dismutase (SOD) activity and malondialdehyde (MDA) levels were measured using SOD and MDA assay kits (Nanjing Jiancheng Bioengineering Institute, Nanjing, China), respectively. Briefly, tissue homogenates were prepared and centrifuged according to the manufacturer's instructions, and the supernatants were collected for analysis. SOD activity was determined using the WST-1 method, while MDA levels were measured using the thiobarbituric acid method. Total cholesterol (TC), triglyceride (TG), low-density lipoprotein cholesterol (LDL-C), high-density lipoprotein cholesterol (HDL-C), and free fatty acid (FFA) levels were measured using corresponding assay kits (R&D Systems, Minneapolis, MN, USA) according to the manufacturer's instructions. Absorbance was measured using a microplate reader, and the results were calculated according to the manufacturer's instructions. Rat glycosylated hemoglobin A1c (GHb) ELISA kit and rat insulin (INS) ELISA kit were obtained from Enzyme-linked Biotechnology, Shanghai, China; Glycogen assay kit was obtained from Solarbio; rat TNF-α ELISA kit was obtained from Absin, Shanghai, China; soluble rat ICAM-1 ELISA kit, rat IL-1β ELISA kit, rat IL-6 ELISA kit, and rat vascular endothelial growth factor (VEGF) ELISA kit were obtained from Boster, Wuhan, China.

Hematoxylin-Eosin Staining The pathological malformations that occurred in the tissue of the retina were determined by utilizing the Hematoxylin and Eosin (HE) Staining Kit (Beyotime, Shanghai, China). Using 4% paraformaldehyde, the tissues of the retina were fixed in 4% paraformaldehyde then embedded in paraffin. The sections of retina tissues were deparaffinized and then hydrated. Hematoxylin solution was used for staining for 5min then finally dipped in eosin solution for 30s. Finally, the sections were observed under BX50 microscope (Olympus, Tokyo, Japan).

Quantitative Reverse Transcription Polymerase Chain Reaction Total RNA extraction from retina tissues or CP-R114 cells was performed utilizing TRIzol reagent (Invitrogen, Carlsbad, CA, USA). To ensure the purity of the RNA, DNase treatment was carried out following RNA extraction to eliminate any residual genomic DNA. The RNA concentration was analyzed using Eppendorf BioPhotometer (Eppendorf, Hamburg, Germany). Total RNA served as a template for synthesizing complementary DNA using PrimeScript™ RT reagent Kit (Takara, Tokyo, Japan). mRNA relative expressions were determined with TB Green® Premix Ex Taq™ II (Takara). The sequences of the primers are as follows (Table 1). Calculations of the results were done using the $2^{-\Delta\Delta CT}$ method.

Western Blotting Using RIPA lysis buffer (Beyotime), retina tissues or CP-R114 cells were lysed to and the concentration of the protein was detected using BCA Protein Assay Kit (Beyotime). Utilizing 10% SDS-PAGE gel electrophoresis, protein samples (25 μg) were separated before they were transferred onto a polyvinylidene difluoride (PVDF) membrane. Following blocking, the membranes were incubated overnight with the primary antibodies; rabbit anti-SAHH (DF7260, 1:500 dilution), rabbit anti-DNMT3b (AF5493,

Table 1 The primer sequences used in qRT-PCR

Gene	Sequence (5′-3′)
H19-F	CTAAGTCGATTGCACTGGTTTGG
H19-R	ACACCCAGTTGCCCTCAGAC
SAHH-F	CTGTGGAGACTGCTGTCCTCATTG
SAHH-R	GTTAGTAAGGTCACCGCCATCATCC
DNMT3b-F	CGGATGATGGAGATGGCTCTGATATTC
DNMT3b-R	AGGCTGGAGATACTGTTGCTGTTTC
β-actin-F	CCCATCTATGAGGGTTACGC
β-actin-R	TTTAATGTCACGCACGATTTC

qRT-PCR: Quantitative reverse transcription polymerase chain reaction; SAHH: S-adenosylhomocysteine hydrolase; DNMT: S-adenosylmethionine-dependent methyltransferases; F: Forward primer; R: Reverse primer.

1:500 dilution), rabbit anti-NLRP3 (DF7438, 1:500 dilution), rabbit anti-apoptosis-associated speck-like protein containing a caspase recruitment domain (ASC; DF6304, 1:500 dilution), rabbit anti-Caspase-1 (AF5418, 1:500 dilution), and rabbit anti-IL-1β (AF5103, 1:500 dilution) antibodies at 4℃. The following day, the membranes were incubated with secondary antibody goat anti-rabbit HRP-IgG antibody (1:5000) for 1h at room temperature. All antibodies were obtained from Affinity Biosciences (Beijing, China). β-actin antibody was used as an internal reference. ImageJ software was employed to detect the protein expression of bands.

Immunofluorescence Analysis Sections of tissues from the retina were fixed with 4% paraformaldehyde and inserted into paraffin. The sections were deparaffinized and then hydrated. After which, 0.5% Triton-X-100 was used to treat the sections for 20min, to block the non-specific sites, the tissue sections were then incubated with normal goat serum. Incubation with SAHH (DF7260, 1:500 dilution), DNMT3b (AF5493, 1:500 dilution), NLRP3 (DF7438, 1:500 dilution), ASC (DF6304, 1:500 dilution), Caspase-1 (AF5418, 1:500 dilution) or IL-1β (AF5103, 1:500 dilution) at 4℃ overnight was performed. Then goat anti-rabbit IgG H&L (DyLight® 488) secondary antibody (1:500 dilution) was added to the membranes and maintained at room temperature for 1h. All antibodies were obtained from Affinity Biosciences, except for the secondary antibody (Abcam, Cambridge, MA, USA). The sections were lastly treated and visualized under an Axiovert200 Inverted fluorescence microscope (Carl-Zeiss Medditec, Jena, Germany).

Statistical Analysis Each experiment was conducted in triplicate. All data have been presented as mean±standard deviation. Statistical analysis was determined using SPSS 22.0 statistical software (IBM, Armonk, NY, USA). The normality of the data was evaluated using the Shapiro-Wilk test. The statistical difference between two groups and multiple groups was calculated using the two-tailed Student's *t* test and one-way analysis of variance (ANOVA) followed by the LSD post hoc test, respectively. Statistical significance was set at $P<0.05$.

RESULTS

H19 Knockout Ameliorated Glucose Metabolism Disorders in DM Rats To elucidate the pathological mechanism of H19 in DR, a DM model of normal and H19-KO rats was constructed. The samples of blood from the rats were analyzed and the body weights measured, and the results expressed no measurable difference in the body weight as well as glucose levels in both WT and the H19-KO rats. In diabetic rats, body weight was significantly reduced, while it was significantly increased in H19-KO diabetic rats compared to WT diabetic rats (Figure 1A). Fasting blood glucose is an important indicator to measure the degree of diabetic symptoms, and it is also an important indicator to reflect the basic function of pancreatic islets[27]. The levels of glucose in the blood were elevated and higher than 7.8 mmol/L in DM rats, which was rescued by H19-KO (Figure 1B). The levels of GHb, INS, muscle glycogen and hepatic glycogen had no changes in normal and H19-KO rats. The levels of GHb were increased, while the levels of INS, muscle glycogen, and hepatic glycogen were decreased in DM rats. H19-KO reduced GHb levels and enhanced the levels of INS, muscle glycogen, and hepatic glycogen in DM rats (Figure 1C–1F). The levels of SOD were reduced and the MDA levels were elevated in DM rats, which were abrogated by H19-KO (Figure 1G–1H).

H19 Knockout Ameliorated Lipid Metabolism Disorders in DM Rats Most type 2 DM patients exhibit abnormal blood lipids, which are marked by significantly raised elevated TGs and LDL-Cs, and decreased HDL-C[29]. Then, we detected the influence of H19-KO on the lipid metabolisms of DM rats. H19-KO had no effect on lipid metabolism-related factors in WT rats. However, TC and TG expressions were raised in DM rats. H19-KO caused lowered levels of TC and TG in DM rats (Figure 2A–2B). Compared with WT rats, DM rats displayed a decreased HDL-C serum level and an increased LDL-C. Inhibition of H19 reversed the impact on HDL-C and LDL-C levels in DM rats (Figure 2C–2D). In addition, FFA levels were elevated in DM rats compared to WT rats. H19-KO reduced FFA levels in DM rats (Figure 2E).

H19 Knockout Alleviated Retinal Tissue Degeneration and Increased SAHH and DNMT3b Expression in DM Rats HE staining showed an intact and continuous endothelial cell without hyperplasia in both WT and H19-KO rats. In contrast, DM rats exhibited a significantly decreased thickness of the outer nuclear layer. Notably, H19-KO effectively alleviated retinal tissue lesions in DM rats (Figure 3A–3B). Moreover, we analyzed the H19, SAHH, and DNMT3b expression levels in the retinal tissues. H19 was not expressed in H19-KO and

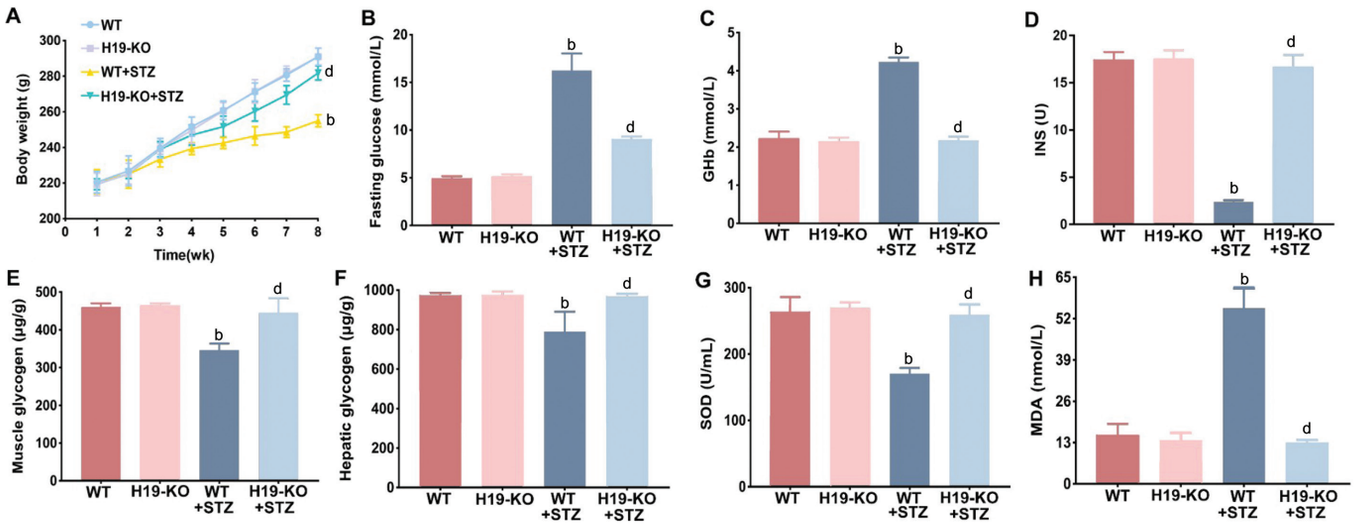


Figure 1 Effect of H19 deficiency on glycometabolism of DM rats DM model of rats was constructed by administration of HFHS diet combined with STZ. WT and H19-KO rats served as control. The weight of the rats was measured (A). The levels of blood glucose (B), GHb (C), INS (D), muscle glycogen (E), hepatic glycogen (F), and the levels of SOD (G), MDA (H) were detected. [b]*P*<0.01 *vs* WT group; [d]*P*<0.01 *vs* WT+STZ group. DM: Diabetes mellitus; WT: Wide type; KO: Knockout; HFHS: High-fat and high-sugar; STZ: Streptozotocin; GHb: Glycosylated hemoglobin A1c; INS: Insulin; SOD: Superoxide dismutase; MDA: Malonaldehyde.

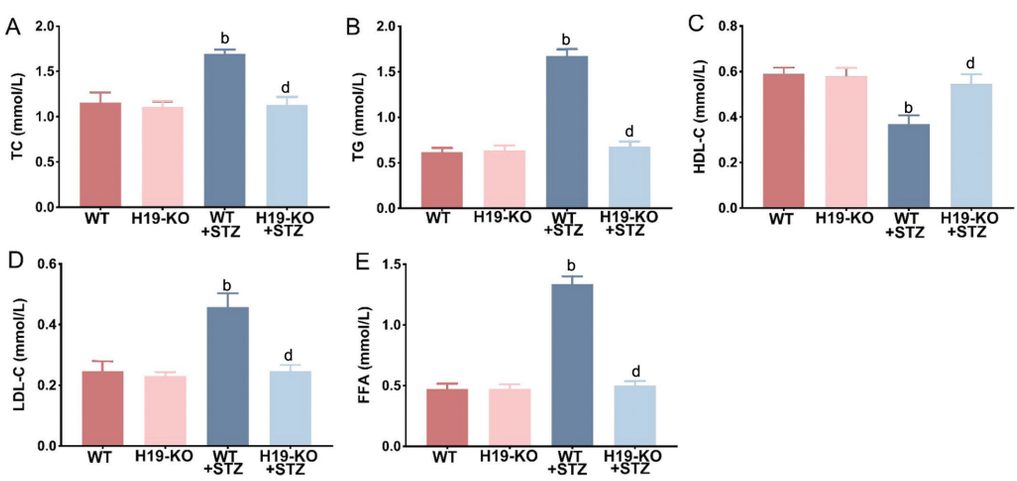


Figure 2 Effect of H19 deficiency on serum lipids of DM rats DM model of rats was constructed by administration of HFHS diet combined with STZ. WT and H19-KO rats served as control. The levels of TC (A), TG (B), HDL-C (C), LDL-C (D), and FFA (E) in the serum of rats were detected. [b]*P*<0.01 *vs* WT group; [d]*P*<0.01 *vs* WT+STZ group. DM: Diabetes mellitus; WT: Wide type; KO: Knockout; HFHS: High-fat and high-sugar; STZ: Streptozotocin; TC: Total cholesterol; TG: Triglyceride; LDL-C: Low-density lipoprotein cholesterol; HDL-C: High-density lipoprotein cholesterol; FFA: Free fatty acid.

H19-KO-STZ rats, while H19 was highly expressed in the DM rats (Figure 3C). DM rats exhibited a down-regulation of SAHH and DNMT3b in retina tissues, which was enhanced by H19-KO (Figure 3D–3E).

H19 Knockout Inhibited Inflammatory Response in DM Rats The results revealed elevated levels of IL-6, IL-1β, and TNF-α in the retinal tissues of DM rats. H19-KO led to a decrease of IL-1β, IL-6, and TNF-α levels in the retina tissues of DM rats (Figure 4A–4C). Raised levels of ICAM-1 and VEGF were also observed in the retina tissues of DM rats and were also inhibited by H19-KO (Figure 4D–4E).

H19 Knockout Enhanced SAHH and DNMT3b Expression and Inhibited NLRP3 Inflammasome in DM Rats Western blot was conducted to examine NLRP3 inflammasome-related protein levels in DM rats. The expression of SAHH and DNMT3b was severely decreased in retina of DM rats. H19-KO caused an up-regulation of SAHH and DNMT3b in DM rats (Figure 5A–5C). DM rats exhibited an increase of NLRP3, ASC, Caspase-1, and IL-1β expression and H19-KO inversed the trend (Figure 5D–5G). Immunofluorescence analysis also revealed that SAHH and DNMT3b were down-regulated, and ASC, NLRP3, IL-1β, and Caspase-1 were up-regulated in retina of DM rats and H19-KO inversed the trend (Figure 6).

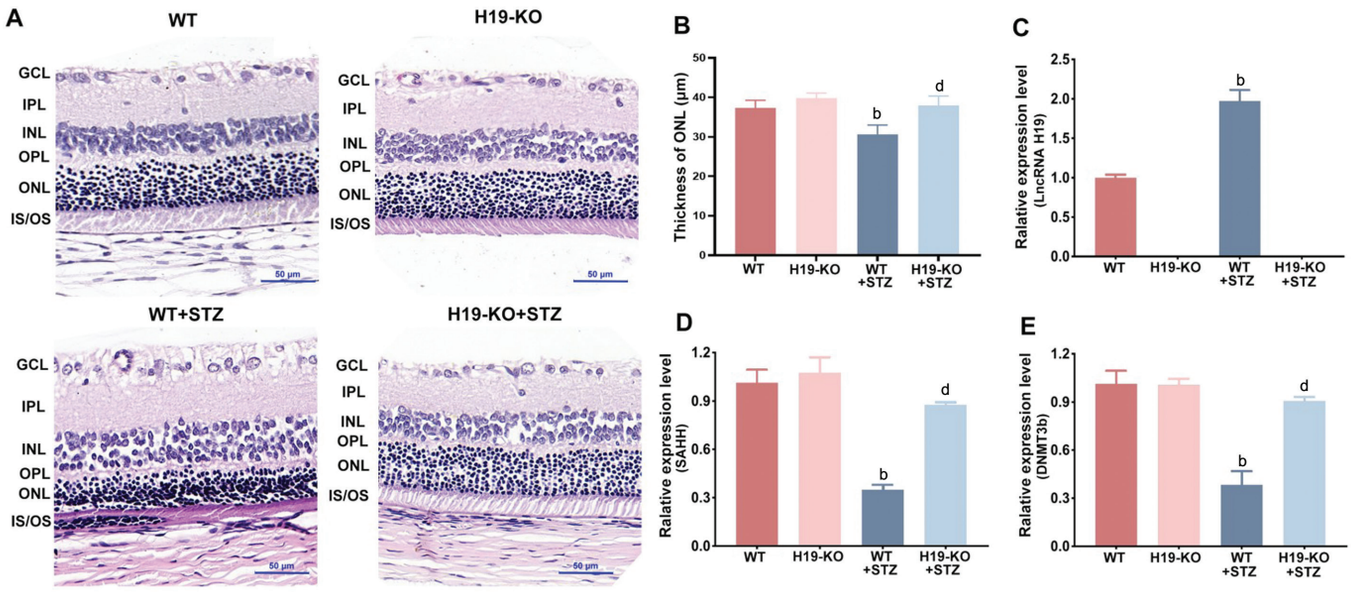


Figure 3 Effect of H19 KO on retina tissue damage, and SAHH and DNMT3b mRNA in DM rats DM model of rats was constructed by administration of HFHS diet combined with STZ. WT and H19-KO rats served as control. HE staining was performed to observe the pathological changes in retina tissues (A) and the thickness of ONL (B), and the expression of H19 (C), SAHH (D), and DNMT3b (E) in retina tissues of rats was assessed by qRT-PCR. ^{b}P<0.01 *vs* WT group; ^{d}P<0.01 *vs* WT+STZ group. DM: Diabetes mellitus; WT: Wide type; KO: Knockout; HFHS: High-fat and high-sugar; STZ: Streptozotocin; GCL: Ganglion cell layer; IPL: Inner plexiform layer; INL: Inner nuclear layer; OPL: Outer plexiform layer; ONL: Outer nuclear layer; IS/OS: Inner segment/outer segment; SAHH: S-adenosylhomocysteine hydrolase; DNMT: S-adenosylmethionine-dependent methyltransferases; qRT-PCR: Quantitative reverse transcription polymerase chain reaction; HE: Hematoxylin and eosin.

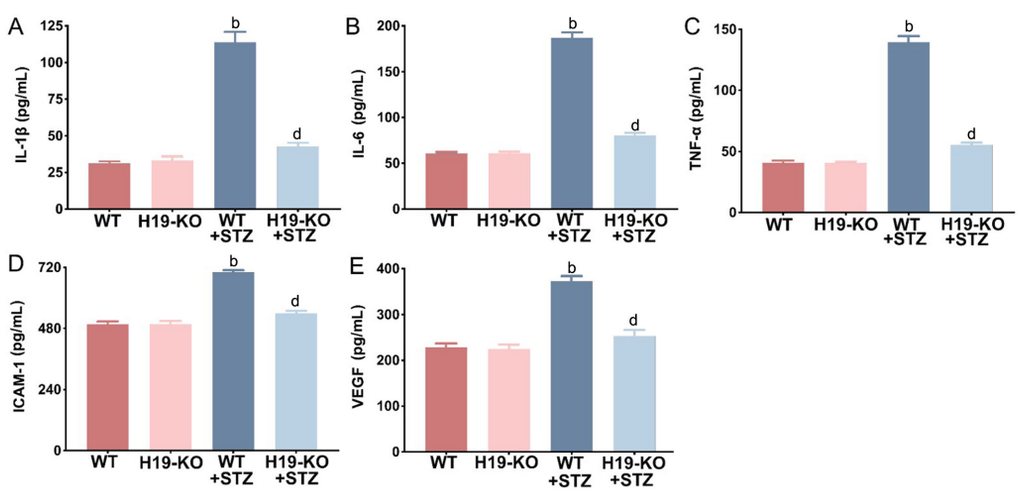


Figure 4 Effect of H19 KO on inflammatory response in DM rats DM model of rats was constructed by administration of HFHS diet combined with STZ. WT and H19-KO rats served as control. The levels of IL-1β (A), IL-6 (B), TNF-α (C), ICAM-1 (D), and VEGF (E) in retina tissues of rats were detected by ELISA. ^{b}P<0.01 *vs* WT group; ^{d}P<0.01 *vs* WT+STZ group. DM: Diabetes mellitus; WT: Wide type; KO: Knockout; HFHS: High-fat and high-sugar; STZ: Streptozotocin; IL: Interleukin; TNF-α: Tumor necrosis factor-alpha; ICAM-1: Intercellular adhesion molecule 1; VEGF: Vascular endothelial growth factor; ELISA: Enzyme-linked immunosorbent assay.

H19 Deficiency Enhanced SAHH and DNMT3b Expression in High Glucose-treated CP-R114 Cells Furthermore, we verified the functional role of H19-KO in DR *in vitro*. CP-R114 cells were treated with high glucose to mimic DM condition. High glucose treatment obviously inhibited the cell survival of CP-R114 cells (Figure 7A). H19 expression was significantly inhibited in CP-R114 cells treated with si-H19 (Figure 7B). Moreover, H19 silencing had no effect on the levels of SOD and MDA. High glucose treatment reduced SOD levels and enhanced MDA levels in CP-R114 cells, which was rescued by H19 silencing (Figure 7C–7D). The expression of H19, SAHH, and DNMT3b in CP-R114 cells were detected by qRT-PCR. H19 deficiency repressed H19 expression in CP-R114 cells, whereas had no influence on SAHH and DNMT3b expression. H19 was up-regulated, and SAHH and DNMT3b were suppressed in CP-R114 cells cultured in high glucose.

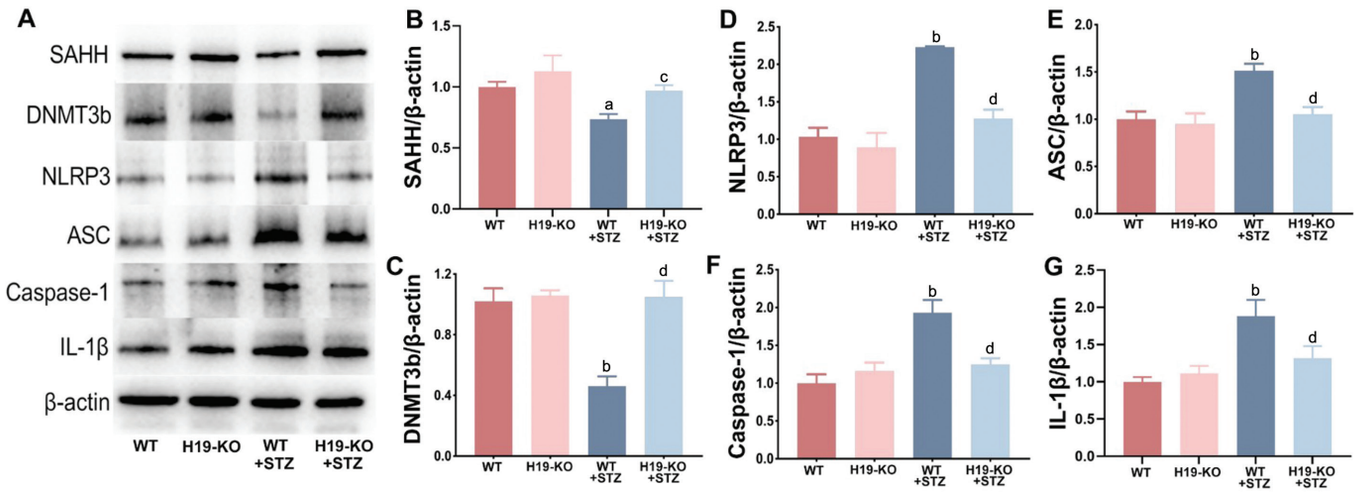


Figure 5 Effect of H19 KO on SAHH and DNMT3b protein expression, and NLRP3 inflammasome in DM rats DM model of rats was constructed by administration of HFHS diet combined with STZ. WT and H19-KO rats served as control. A: Western blotting was carried out to examine the expression of SAHH (B), DNMT3b (C), NLRP3 (D), ASC (E), Caspase-1 (F), and IL-1β (G) in retina tissues of rats. [a]*P*<0.05, [b]*P*<0.01 *vs* WT group; [c]*P*<0.05, [d]*P*<0.01 *vs* WT+STZ group. DM: Diabetes mellitus; WT: Wide type; KO: Knockout; HFHS: High-fat and high-sugar; STZ: Streptozotocin; SAHH: S-adenosylhomocysteine hydrolase; DNMT: S-adenosylmethionine-dependent methyltransferases; NLRP3: NLR family pyrin domain containing 3; ASC: Apoptosis-associated speck-like protein containing a caspase recruitment domain; IL: Interleukin.

H19 silencing abrogated the high glucose-mediated promotion of H19 and inhibition of SAHH and DNMT3b expression in CP-R114 cells (Figure 7E–7G).

H19 Deficiency Inhibited Inflammatory Response in High Glucose-treated CP-R114 Cells H19 deficiency impaired high glucose-induced increase of IL-1β, IL-6 as well as TNF-α levels in CP-R114 cells (Figure 8A–8C). The expressions of ICAM-1 and VEGF were elevated in CP-R114 cells following high glucose treatment and suppressed in high glucose treatment combined with si-H19 (Figure 8D–8E).

H19 Deficiency Inhibited NLRP3 Inflammasome in High Glucose-treated CP-R114 Cells Finally, the influence of H19 deficiency on NLRP3 inflammasome in CP-R114 cells was detected using Western blot analysis. The expressions of SAHH and DNMT3b were severely down-regulated in CP-R114 cells cultured in high glucose conditions. H19 deficiency caused an elevation of SAHH and DNMT3b in CP-R114 cells cultured in high glucose treatment (Figure 9A–9C). Additionally, high glucose treatment caused an increase of NLRP3, ASC, Caspase-1, and IL-1β expression in CP-R114 cells. The influence conferred by high glucose was abolished by H19 silencing (Figure 9D–9G).

DISCUSSION

DR is a major contributor to vision loss in adults, which seriously threatens the health of humans. This work found that H19-KO improved glucose metabolism and lipid metabolism disorders, as well as repressed the occurrence of oxidative stress in DM rats. Importantly, H19-KO alleviated the retina tissue damage and enhanced the expression of SAHH and DNMT3b in DM rats. The expressions of inflammatory factors, VEGF, and ICAM-1 were decreased in H19-KO DM rats. NLRP3 inflammasome-related protein levels in DM rats were also repressed by H19 deficiency. Consistently, H19 deficiency repressed NLRP3 inflammasome and enhanced SAHH and DNMT3b expression in high glucose-treated CP-R114 cells. In summary, H19 knockout activated the SAHH/DNMT3b pathway and repressed NLRP3 inflammasome, which contributed to alleviating DR progression in rats (Figure 10).

H19 has a vital function in various diseases, such as cardiac hypertrophy, cancers, osteoporosis, and DM[30-33]. Inhibition of H19 represses hippocampal neuron apoptosis and STZ-induced oxidative stress in DM rats by reducing the insulin-like growth factor 2 (IGF2) methylation levels[34]. H19-KO suppresses atypical differentiation pattens of epithelial cells in the intestine of DM mice through regulating miR-141-3p/β-catenin axis[35]. Research have shown that H19 plays a complex role in metabolic diseases. In diabetic mice and patients, H19 was reduced in skeletal muscle, leading to increased histone deacetylase 6 levels and impaired insulin signaling[36]. Conversely, obesity and high-fat diets were associated with elevated H19 expression, which promotes lipid accumulation and insulin resistance. Silencing H19 can improve glucose metabolism and reduce lipid levels[37-39]. Consistently, we also found that H19 exhibited a considerably high level of expression in retinal tissues of DM rats as well as in CP-R114 cells cultured with high glucose conditions. H19-KO improved the glycose metabolism and lipid metabolism disorders and repressed oxidative stress and retina tissue damage in DM rats. Moreover, it is speculated that H19 may

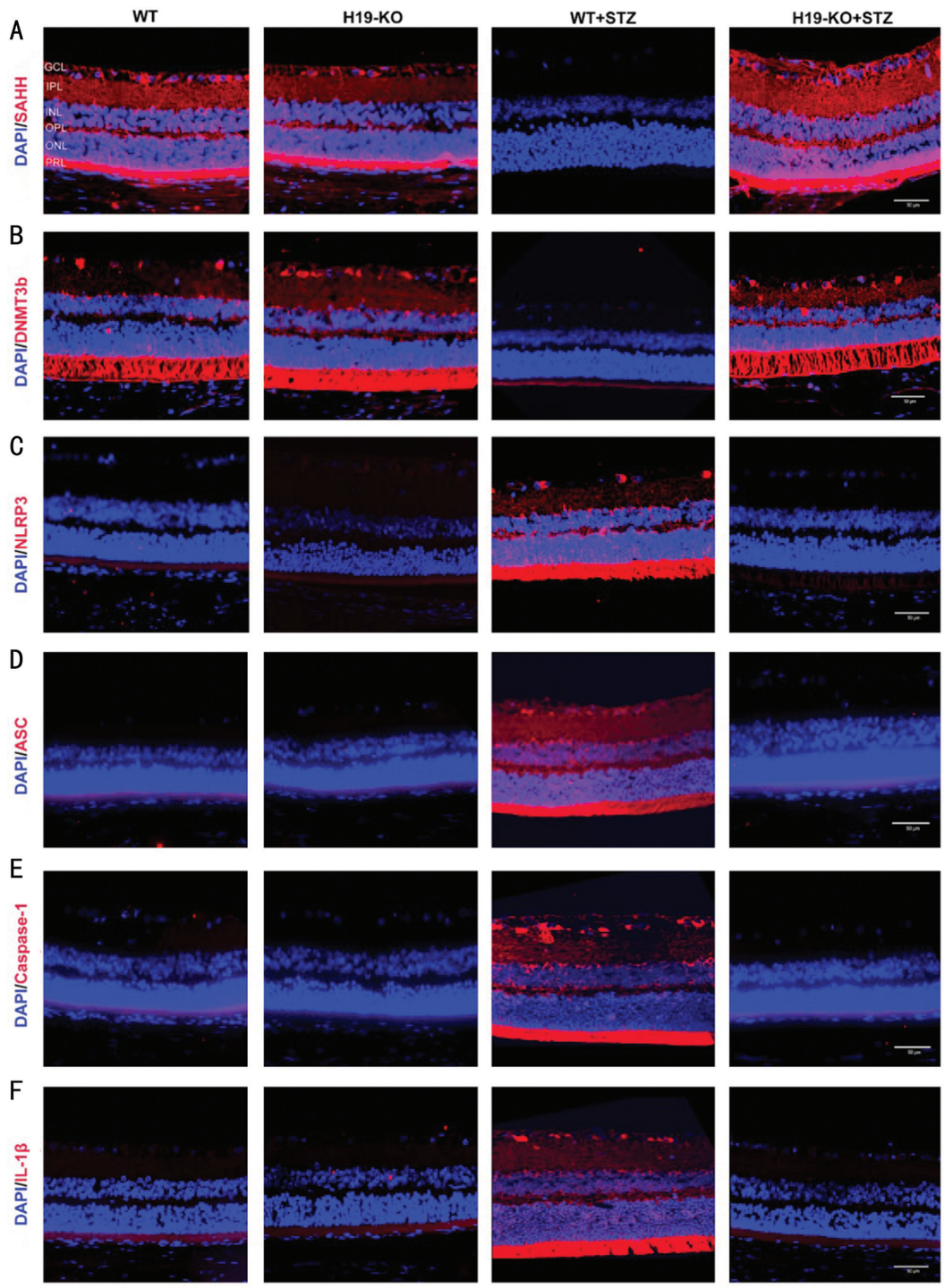


Figure 6 Influence of H19 knockout on the expression of SAHH, DNMT3b, and NLRP3 inflammasome in DM rats DM model of rats was constructed by administration of HFHS diet combined with STZ. WT and H19-KO rats served as control. Immunofluorescence analysis was carried out to examine the expression of SAHH (A), DNMT3b (B), NLRP3 (C), ASC (D), Caspase-1 (E), and IL-1β (F) in retina tissues of rats. DM: Diabetes mellitus; WT: Wide type; KO: Knockout; HFHS: High-fat and high-sugar; STZ: Streptozotocin; SAHH: S-adenosylhomocysteine hydrolase; DNMT: S-adenosylmethionine-dependent methyltransferases; NLRP3: NLR family pyrin domain containing 3; ASC: Apoptosis-associated speck-like protein containing a caspase recruitment domain; IL: Interleukin.

exert abnormal effects through specific metabolic pathways under high glucose conditions, as the expression levels of SAHH and DNMT3B remain unchanged in the presence of H19-KO or inhibition under normal glucose condition. It is suggested that the suppression of SAHH and DNMT3B expression in high glucose condition may be mediated through H19-induced epigenetic mechanisms, such as DNA methylation or histone modification. The specific mechanisms underlying this phenomenon require further investigation for a more comprehensive understanding. However, there are

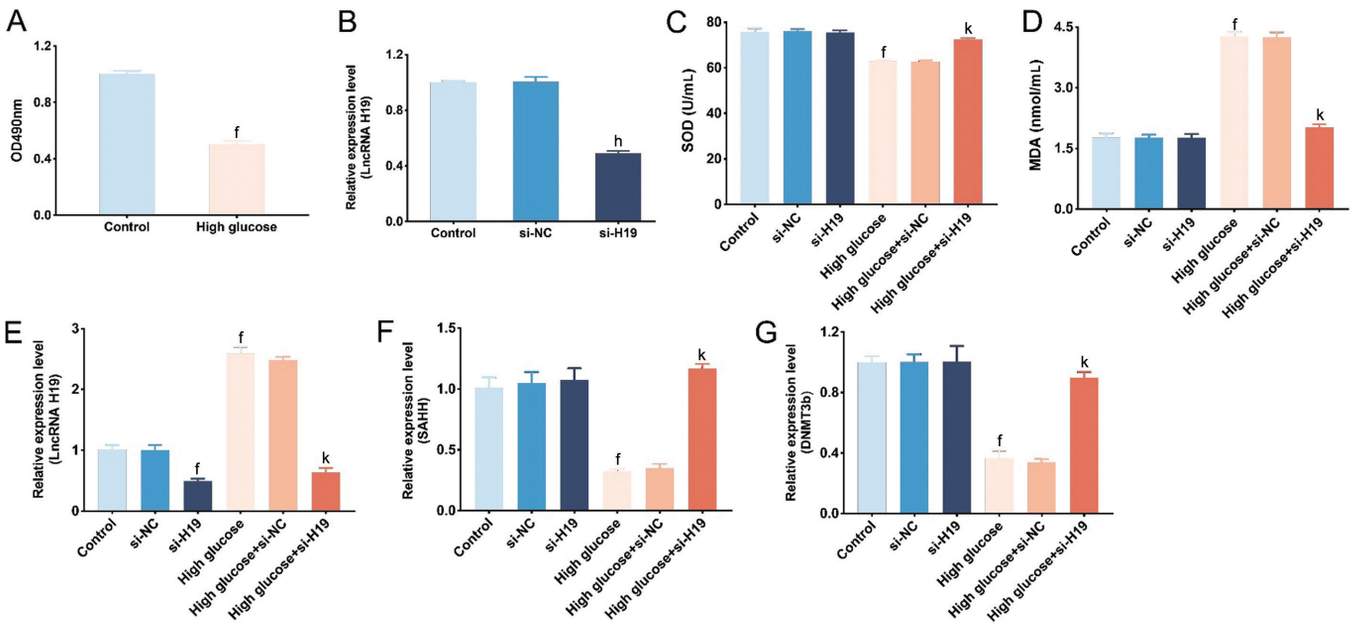


Figure 7 Effect of H19 deficiency on SAHH and DNMT3b expression in high glucose-treated CP-R114 cells A: MTS assay was performed to assess cell survival of CP-R114 cells following high glucose treatment; B: The qRT-PCR was carried out to detect the expression of H19 in the CP-R114 cells following transfection of si-H19 or si-NC. C–G: CP-R114 cells were transfected with si-H19 or si-NC, followed by high glucose treatment. The levels of SOD (C) and MDA (D) in the CP-R114 cells were examined. The expression of H19 (E), SAHH (F), and DNMT3b (G) in the CP-R114 cells was measured by qRT-PCR. ^{f}P<0.01 *vs* control group; ^{h}P<0.01 *vs* si-NC group; ^{k}P<0.01 *vs* high glucose+si-NC group. SAHH: S-adenosylhomocysteine hydrolase; DNMT: S-adenosylmethionine-dependent methyltransferases; CP-R114: Rat retinal microvascular endothelial cells; MTS: 3-(4,5-dimethylthiazol-2-yl)-5-(3-carboxymethoxyphenyl)-2-(4-sulfophenyl)-2H-tetrazolium; qRT-PCR: Quantitative reverse transcription polymerase chain reaction; si-H19: H19 small interfering RNA; si-NC: Negative control small interfering RNA; SOD: Superoxide dismutase; MDA: Malonaldehyde.

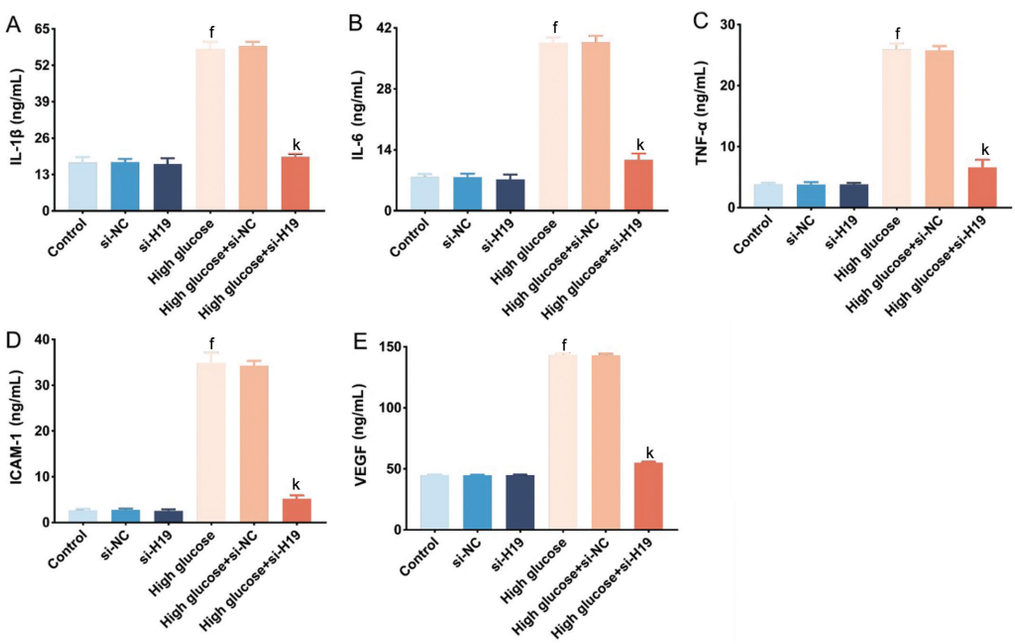


Figure 8 Effect of H19 KO on inflammatory factors in high glucose-treated CP-R114 cells CP-R114 cells were transfected with si-H19 or si-NC, followed by high glucose treatment. The levels of IL-1β (A), IL-6 (B), TNF-α (C), ICAM-1 (D), and VEGF (E) in the CP-R114 cells were detected by ELISA. ^{f}P<0.01 *vs* control group; ^{k}P<0.01 *vs* high glucose+si-NC group. KO: Knockout; CP-R114: Rat retinal microvascular endothelial cells; si-H19: H19 small interfering RNA; si-NC: Negative control small interfering RNA; IL: Interleukin; TNF-α: Tumor necrosis factor-alpha; ICAM-1: Intercellular adhesion molecule 1; VEGF: Vascular endothelial growth factor; ELISA: Enzyme-linked immunosorbent assay.

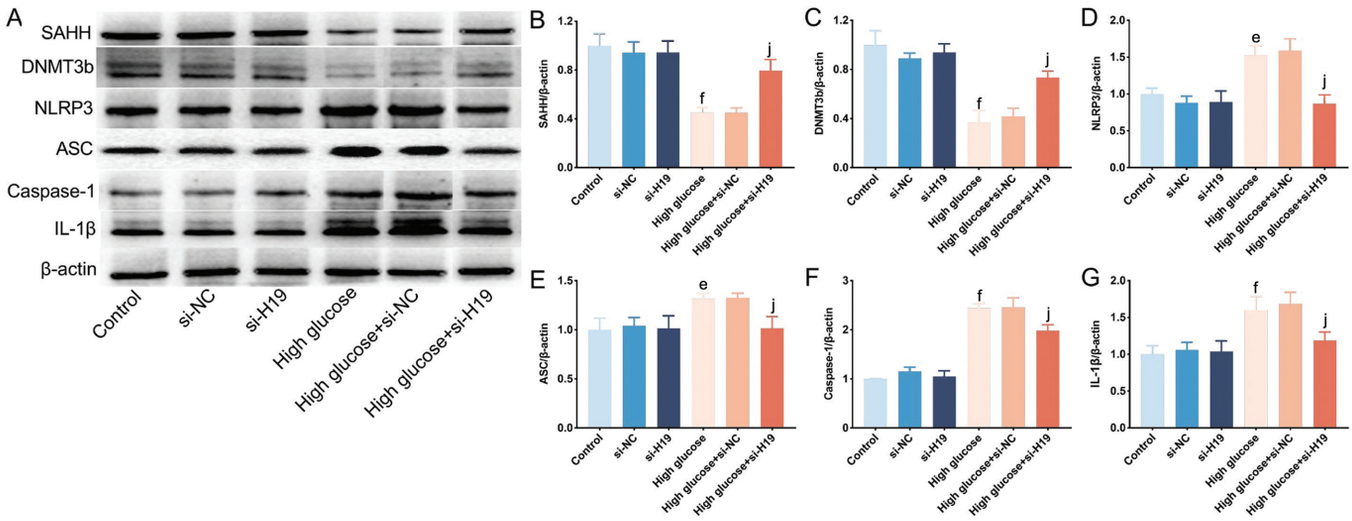


Figure 9 Effect of H19 KO on NLRP3 inflammasome in high glucose-treated CP-R114 cells CP-R114 cells were transfected with si-H19 or si-NC, followed by high glucose treatment. Western blotting (A) was carried out to examine the expression of SAHH (B), DNMT3b (C), NLRP3 (D), ASC (E), Caspase-1 (F), and IL-1β (G) in CP-R114 cells. $^{e}P<0.05$, $^{f}P<0.01$ *vs* control group; $^{j}P<0.05$ *vs* high glucose+si-NC group. KO: Knockout; NLRP3: NLR family pyrin domain containing 3; CP-R114: Rat retinal microvascular endothelial cells; si-H19: H19 small interfering RNA; si-NC: Negative control small interfering RNA; SAHH: S-adenosylhomocysteine hydrolase; DNMT: S-adenosylmethionine-dependent methyltransferases; ASC: Apoptosis-associated speck-like protein containing a caspase recruitment domain; IL: Interleukin.

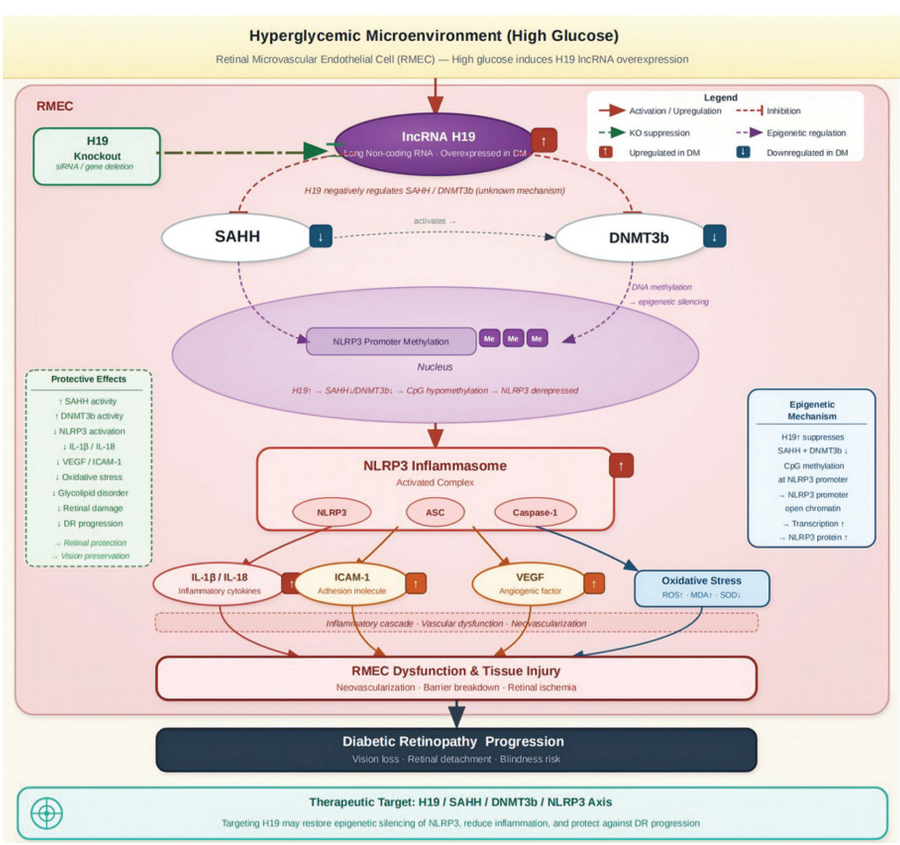


Figure 10 Mechanism of the lncRNA H19/SAHH/DNMT3b/NLRP3 axis in DR Hyperglycemia upregulates lncRNA H19 in RMECs. H19 suppresses SAHH and DNMT3b, relieving their epigenetic regulation on NLRP3 and resulting in inflammasome activation. This activation promotes the release of IL-1β/IL-18 and upregulates ICAM-1/VEGF, triggering oxidative stress and inflammation that lead to RMEC dysfunction, neovascularization, and tissue damage. Conversely, H19 knockout restores SAHH/DNMT3b activity, suppresses NLRP3, and exerts protective effects. lncRNA: Long non-coding RNA; SAHH: S-adenosylhomocysteine hydrolase; DNMT: S-adenosylmethionine-dependent methyltransferases; NLRP3: NLR family pyrin domain containing 3; DR: Diabetic retinopathy; RMECs: Retinal microvascular endothelial cells; IL: Interleukin; ICAM-1: Intercellular adhesion molecule 1; VEGF: Vascular endothelial growth factor.

also different studies. Thomas *et al*[22] revealed that H19 levels were suppressed in human retinal endothelial cells incubated in high glucose conditions and its overexpression prevented endothelial-mesenchymal transition in DR. H19 is suppressed in adult retinal pigment epithelial cell line-19 (ARPE-19) incubated in high glucose conditions, and H19 silencing represses high glucose-induced inflammation in ARPE-19 cells through modulating miR-19b/SIRT1 or miR-93/XBP1s axis[20-21]. Animal models and cell models cannot fully simulate the pathological conditions in the organism. Different cell models may cause changes in the expression and functional role of H19. Thus, the biological function of H19 in DR is still controversial and requires extensive study.

Some previous studies have identified that inhibiting SAHH by adenosine dialdehyde activates NLRP3 inflammasome, promotes podocyte injury induced by high glucose levels, and exacerbates STZ-induced diabetic nephropathy[40-41]. The inhibition of SAHH exacerbated diabetic nephropathy through regulating EZH2/EGR1/TXNIP/NLRP3 signaling cascade[42]. SAHH has been reported as suppressing in esophageal squamous cell carcinoma cells, it accelerates apoptosis and represses the invasiveness of esophageal squamous cell carcinoma cells[43]. SAHH is abnormally expressed in colorectal cancer and hence can be targeted for the screening of colorectal cancer as a biomarker[44]. H19 interacts with SAHH and inhibits the function of SAHH, thereby increasing the accumulation of SAH. SAH, as an inhibitor of DNMT3b, can bind to DNMT3b and reduce the levels of methylation of genomic DNA. When the levels of H19 are low, SAHH can hydrolyze SAH, causing SAH to release DNMT3b, which enhances the methylation levels of DNA[23,26]. This research demonstrated that H19 deficiency enhanced SAHH and DNMT3b expression in DM rats and high glucose-treated CP-R114 cells. These data indicated that H19 deficiency may affect DR progression by regulating the SAHH/DNMT3b pathway.

NLRP3 inflammasome possesses a fundamental in the advancement of DR[45-46]. Inhibition of NLRP3 inflammasome by its inhibitor Mcc950 can reduce the permeability of blood vessels, thereby haltering the advancement of DR in mice[47-48]. NLRP3 inflammasome is activated in DM rats, minocycline inhibits NLRP3 inflammasome activation and represses retinal blood vessel permeability and cellular apoptosis[49]. Consistently, this work revealed that NLRP3 inflammasome was activated in DM rats and in CP-R114 cells cultured in high glucose conditions. H19 deficiency suppressed NLRP3 inflammasome in DM rats and high glucose-treated CP-R114 cells, thereby alleviating the progression of DR.

This study reveal that H19-KO activates SAHH/DNMT3b pathway and represses NLRP3 inflammasome, which alleviates DR progression in rats. Therefore, H19 may be a promising avenue of study for DR treatment.

ACKNOWLEDGEMENTS

Authors' Contributions: Chen H: Conceptualization, methodology, investigation, and writing original draft; Pang YH: Data curation, formal analysis, methodology, and writing original draft; Zhang XZ, Liao NY, Li ML, Ji YY: Methodology, validation, and supervision; Mi L, Gan YH, Su YY: Investigation, experimental, data collection and validation; Wen F: Conceptualization, supervision, project administration, review and editing.

Data Availability Statement: The original experimental data generated during this study are available from the corresponding author upon reasonable request.

AI-Generated Content Disclosure: No artificial intelligence (AI) tools were used for this work.

Foundations: Supported by National Natural Science Foundation of China (No.81970813; No.82571234); Natural Science Foundation of Guangdong Province (No.2023A1515011198); Guangzhou Municipal Science and Technology Program (No.SL2023A03J00553).

Conflicts of Interest: Chen H, None; **Pang YH,** None; **Zhang XZ,** None; **Liao NY,** None; **Li ML,** None; **Ji YY,** None; **Mi L,** None; **Gan YH,** None; **Su YY,** None; **Wen F,** None.

REFERENCES

1 Tarr JM, Kaul K, Chopra M, *et al*. Pathophysiology of diabetic retinopathy. *ISRN Ophthalmol* 2013;2013:343560.

2 ElSayed NA, Aleppo G, Aroda VR, *et al*. 2. Classification and diagnosis of diabetes: Standards of care in diabetes-2023. *Diabetes Care* 2023;46(Suppl 1):S19-S40.

3 Tuttle KR, Jones CR, Daratha KB, *et al*. Incidence of chronic kidney disease among adults with diabetes, 2015-2020. *N Engl J Med* 2022;387(15):1430-1431.

4 Wong ND, Sattar N. Cardiovascular risk in diabetes mellitus: epidemiology, assessment and prevention. *Nat Rev Cardiol* 2023;20(10):685-695.

5 Khan A, Petropoulos IN, Ponirakis G, *et al*. Visual complications in diabetes mellitus: beyond retinopathy. *Diabet Med* 2017;34(4): 478-484.

6 El Khalili L, El Khalili L, Rawshani A, *et al*. Cardiometabolic risk factors and disease trends for atrial fibrillation in individuals with type 1 diabetes: a nationwide registry study. *Cardiovasc Diabetol* 2025;24(1):117.

7 Bourne RR, Stevens GA, White RA, *et al*. Causes of vision loss worldwide, 1990-2010: a systematic analysis. *Lancet Glob Health* 2013;1(6):e339-e349.

8 Antonetti DA, Silva PS, Stitt AW. Current understanding of the molecular and cellular pathology of diabetic retinopathy. *Nat Rev Endocrinol* 2021;17(4):195-206. Erratum in: *Nat Rev Endocrinol* 2025;21(1):62.

9 Invernizzi A, Chhablani J, Viola F, *et al*. Diabetic retinopathy in the pediatric population: pathophysiology, screening, current and future treatments. *Pharmacol Res* 2023;188:106670.

10 Tang L, Xu GT, Zhang JF. Inflammation in diabetic retinopathy: possible roles in pathogenesis and potential implications for therapy. *Neural Regen Res* 2023;18(5):976-982.

11 Thounaojam MC, Montemari A, Powell FL, *et al*. Monosodium urate contributes to retinal inflammation and progression of diabetic retinopathy. *Diabetes* 2019;68(5):1014-1025.

12 Fu S, Zheng Y, Sun Y, *et al*. Suppressing long noncoding RNA OGRU ameliorates diabetic retinopathy by inhibition of oxidative stress and inflammation *via* miR-320/USP14 axis. *Free Radic Biol Med* 2021;169:361-381.

13 Kelley N, Jeltema D, Duan Y, *et al*. The NLRP3 inflammasome: an overview of mechanisms of activation and regulation. *Int J Mol Sci* 2019;20(13):3328.

14 Chaurasia SS, Lim RR, Parikh BH, *et al*. The NLRP3 inflammasome may contribute to pathologic neovascularization in the advanced stages of diabetic retinopathy. *Sci Rep* 2018;8(1):2847.

15 Chai G, Liu S, Yang H, *et al*. NLRP3 blockade suppresses pro-inflammatory and pro-angiogenic cytokine secretion in diabetic retinopathy. *Diabetes Metab Syndr Obes* 2020;13:3047-3058.

16 Ye L, Guo H, Wang Y, *et al*. Exosomal circEhmt1 released from hypoxia-pretreated pericytes regulates high glucose-induced microvascular dysfunction *via* the NFIA/NLRP3 pathway. *Oxid Med Cell Longev* 2021;2021:8833098.

17 Dykes IM, Emanueli C. Transcriptional and post-transcriptional gene regulation by long non-coding RNA. *Genomics Proteomics Bioinformatics* 2017;15(3):177-186.

18 Ilieva MS. Non-coding RNAs in neurological and neuropsychiatric disorders: unraveling the hidden players in disease pathogenesis. *Cells* 2024;13(12):1063.

19 Ghafouri-Fard S, Esmaeili M, Taheri M. H19 lncRNA: roles in tumorigenesis. *Biomed Pharmacother* 2020;123:109774.

20 Luo R, Xiao F, Wang P, *et al*. lncRNA H19 sponging miR-93 to regulate inflammation in retinal epithelial cells under hyperglycemia *via* XBP1s. *Inflamm Res* 2020;69(3):255-265.

21 Luo R, Li L, Hu YX, *et al*. LncRNA H19 inhibits high glucose-induced inflammatory responses of human retinal epithelial cells by targeting miR-19b to increase SIRT1 expression. *Kaohsiung J Med Sci* 2021;37(2):101-110.

22 Thomas AA, Biswas S, Feng B, *et al*. lncRNA H19 prevents endothelial–mesenchymal transition in diabetic retinopathy. *Diabetologia* 2019;62(3):517-530.

23 Zhou J, Yang L, Zhong T, *et al*. H19 lncRNA alters DNA methylation genome wide by regulating S-adenosylhomocysteine hydrolase. *Nat Commun* 2015;6:10221.

24 Deng J, Mueller M, Geng T, *et al*. H19 lncRNA alters methylation and expression of Hnf4α in the liver of metformin-exposed fetuses. *Cell Death Dis* 2017;8(12):e3175.

25 Zhong T, Men Y, Lu L, *et al*. Metformin alters DNA methylation genome-wide *via* the H19/SAHH axis. *Oncogene* 2017;36(17):2345-2354.

26 Zeng L, Sun S, Han D, *et al*. Long non-coding RNA H19/SAHH axis epigenetically regulates odontogenic differentiation of human dental pulp stem cells. *Cell Signal* 2018;52:65-73.

27 Zhang Q, Zhao G, Yang N, *et al*. Fasting blood glucose levels in patients with different types of diseases. *Glycans and Glycosaminoglycans as Clinical Biomarkers and Therapeutics-Part A*. Amsterdam: Elsevier; 2019:277-292.

28 Dai X, Liu S, Cheng L, *et al*. Epigenetic upregulation of H19 and AMPK inhibition concurrently contribute to S-adenosylhomocysteine hydrolase deficiency-promoted atherosclerotic calcification. *Circ Res* 2022;130(10):1565-1582.

29 Ali F, Jamil H, Anwar SS, *et al*. Characterization of lipid parameters in diabetic and non-diabetic atherosclerotic patients. *J Geriatr Cardiol* 2015;12(1):37-43.

30 Su W, Huo Q, Wu H, *et al*. The function of LncRNA-H19 in cardiac hypertrophy. *Cell Biosci* 2021;11(1):153.

31 Shermane Lim YW, Xiang X, Garg M, *et al*. The double-edged sword of H19 lncRNA: insights into cancer therapy. *Cancer Lett* 2021;500:253-262.

32 Chen S, Liu D, Zhou Z, *et al*. Role of long non-coding RNA H19 in the development of osteoporosis. *Mol Med* 2021;27(1):122.

33 Ghaedi H, Zare A, Omrani MD, *et al*. Genetic variants in long noncoding RNA H19 and MEG3 confer risk of type 2 diabetes in an Iranian population. *Gene* 2018;675:265-271.

34 Yu J, Li C, Che L, *et al*. Downregulation of long noncoding RNA H19 rescues hippocampal neurons from apoptosis and oxidative stress by inhibiting IGF2 methylation in mice with streptozotocin-induced diabetes mellitus. *J Cell Physiol* 2019;234(7):10655-10670.

35 Shan TD, Lv SY, Tian ZB, *et al*. Knockdown of lncRNA H19 inhibits abnormal differentiation of small intestinal epithelial cells in diabetic mice. *J Cell Physiol* 2018;234(1):837-848.

36 Kumar A, Datta M. H19 inhibition increases HDAC6 and regulates IRS1 levels and insulin signaling in the skeletal muscle during diabetes. *Mol Med* 2022;28(1):81.

37 Daneshmoghadam J, Omidifar A, Akbari Dilmaghani N, *et al*. The gene expression of long non-coding RNAs (lncRNAs): MEG3 and H19 in adipose tissues from obese women and its association with insulin resistance and obesity indices. *J Clin Lab Anal* 2021;35(5):e23741.

38 Schmidt E, Dhaouadi I, Gaziano I, *et al*. LincRNA H19 protects from dietary obesity by constraining expression of monoallelic genes in brown fat. *Nat Commun* 2018;9(1):3622.

39 Shkurat TP, Ammar M, Bocharova O, *et al*. The role of genetic variants in the long non-coding RNA genes MALAT1 and H19 in the pathogenesis of childhood obesity. *Noncoding RNA* 2023;9(2):22.

40 Shahzad K, Fatima S, Khawaja H, *et al*. Podocyte-specific NLRP3 inflammasome activation promotes diabetic kidney disease. *Kidney Int* 2022;102(4):766-779.

41 Lassén E, Bouchareb R, Daehn IS. Podocyte as the link between sterile inflammation and diabetic kidney disease. *Kidney Int* 2022;102(4):688-690.

42 Dai X, Liao R, Liu C, *et al*. Epigenetic regulation of TXNIP-mediated oxidative stress and NLRP3 inflammasome activation contributes to SAHH inhibition-aggravated diabetic nephropathy. *Redox Biol* 2021;45:102033.

43 Li Q, Mao L, Wang R, *et al*. Overexpression of S-adenosylhomocysteine hydrolase (SAHH) in esophageal squamous cell carcinoma (ESCC) cell lines: effects on apoptosis, migration and adhesion of cells. *Mol Biol Rep* 2014;41(4):2409-2417.

44 Tang M, Zeng L, Zeng Z, *et al*. Proteomics study of colorectal cancer and adenomatous polyps identifies TFR1, SAHH, and HV307 as potential biomarkers for screening. *J Proteomics* 2021; 243:104246.

45 Zheng X, Wan J, Tan G. The mechanisms of NLRP3 inflammasome/pyroptosis activation and their role in diabetic retinopathy. *Front Immunol* 2023;14:1151185.

46 Yang Y, Jiang G, Huang R, *et al*. Targeting the NLRP3 inflammasome in diabetic retinopathy: from pathogenesis to therapeutic strategies. *Biochem Pharmacol* 2023;212:115569.

47 Ge K, Wang Y, Li P, *et al*. Down-expression of the NLRP3 inflammasome delays the progression of diabetic retinopathy. *Microvasc Res* 2022;139:104265.

48 Cai G, Song X, Luo H, *et al*. NLRP3 blockade by MCC950 suppressed osteoclastogenesis *via* NF-κB/c-Fos/NFATc1 signal pathway and alleviated bone loss in diabetes mellitus. *Mol Cell Endocrinol* 2024;594:112382.

49 Chen W, Zhao M, Zhao S, *et al*. Activation of the TXNIP/NLRP3 inflammasome pathway contributes to inflammation in diabetic retinopathy: a novel inhibitory effect of minocycline. *Inflamm Res* 2017;66(2):157-166.